Composite Structures 153 (2016) 42–49

Contents lists available at ScienceDirect

Composite Structures

journal homepage: www.elsevier.com/locate/compstruct

Estimation of transverse shear force during slamming impacts on a simply supported composite panel using a strain derivative method

T. Allen *, M. Battley

Centre for Advanced Composite Materials, The University of Auckland, Private Bag 92019, Auckland 1142, New Zealand

ARTICLE INFO

Article history:
Received 10 December 2015
Accepted 1 June 2016
Available online 2 June 2016

Keywords:
Slamming
Sandwich composites
Transverse shear force
Hydroelasticity
Water impact
Strain measurement

ABSTRACT

Use of sandwich constructions in slamming regions of high speed marine craft has led to increased consideration of the applied transverse shear force. Low shear strength core materials can lead to transverse shear failure becoming a high risk failure mode. Direct measurement of transverse shear force is difficult without altering the structure of the hull panels. This work utilises a non-invasive strain derivative method to estimate the applied transverse shear force. The basis of this method is the correlation between applied bending moment, determined from surface mounted strain gauges, and transverse shear force. A simply supported 1000 × 500 mm instrumented sandwich panel has been tested in the Servo-hydraulic Slam Testing System. Impacts have been undertaken at 10° with vertical velocities from 1.0 to 3.5 m/s. The shear force to bending moment ratio has been compared with the ratio based on a uniformly distributed load, as frequently used in design. An increase of up to 68% for the slamming experiments is observed. This significant difference illustrates a greater applied transverse shear force in slamming regions than would be predicted through the application of a uniformly distributed load.

1. Introduction

Pressures generated during slamming events are one of the most significant load cases for high speed craft. These pressures are generated during the dynamic impact of the hull of a vessel into the free surface of the water. Designers need an efficient process for establishing the required stiffness and strength of a hull structure. This is typically approached either by applying the guidelines as defined by class authorities or by utilising an in-house design methodology. In the majority of cases determining an appropriate slamming pressure load involves equating the anticipated non-uniform dynamic pressure to a uniform static pressure. For example the formula for calculating the magnitude of the equivalent uniform pressure for high speed light craft given by Det Norske Veritas is shown in Eq. (1) [1]. Of note is the fact that the water impact velocity is not considered, rather the design vertical acceleration of the longitudinal centre of gravity.

$$P_{DNV} = 1.3k_1\left(\frac{\Delta}{nA}\right)^{0.3} T_0^{0.7}\frac{50-\beta_x}{50-\beta_{cg}}a_{cg} \tag{1}$$

It is difficult to compare a single impact with the specifications given by class authorities due to this use of acceleration rather than impact velocity in the calculations. Furthermore most scantlings from class authorities must be assessed in their entirety, rather than selecting a single parameter to compare, such as the slamming pressure.

Another option for comparison with results from single experimental impacts is predictions based on theoretical pressures. Established solutions for wedge impacts such as those based on the work of Wagner [2] or von Karman [3], given in Eqs. (2) and (3), can be used. In these solutions the average pressure increases with increasing impact velocity and decreasing deadrise angle.

$$P_{W,ave} = \frac{\rho\pi^2 v^2}{4\tan\beta\cos\beta} \tag{2}$$

$$P_{vK,ave} = \frac{\rho\pi v^2}{2\tan\beta\cos\beta} \tag{3}$$

Experimental values for transverse shear force and bending moment can be used to evaluate the ability of uniform pressure design methodologies, such as those specified by class authorities to predict shear and bending loads during slamming impacts.

Direct measurement of the transverse shear force is difficult experimentally, especially dynamically. Previously researchers have used invasive methods such as shear strain plugs [4] and

* Corresponding author.
E-mail address: Tom.allen@auckland.ac.nz (T. Allen).

http://dx.doi.org/10.1016/j.compstruct.2016.06.001
0263-8223/

Nomenclature

D	flexural rigidity [Nm]	v	vertical velocity [m/s]
M	bending moment [Nm]	ρ	density [kg/m^3]
T	shear force [N]	Δ	displacement-tonnes
ε	strain [m/m]	k_1	longitudinal distribution factor
z	distance to strain gauge from neutral axis [m]	n	number of hulls
d	distance between the neutral axes of sandwich skins [m]	L	vessel length [m]
Δx	distance between centre of two strain gauges [m]	T_0	draught at L/2 [m]
q	uniform Pressure Magnitude [kPa]	β_x	deadrise of transverse section [°]
a	panel width [m]	β_{cg}	deadrise of centre of gravity [°]
b	panel length [m]	α_{cg}	design vertical acceleration of centre of gravity [°]
β	deadrise angle [°]		

shear rods [5]. These both require drilling holes into the core material which may lead to stress concentrations and unexpected variations in structural performance. For this work a non-invasive strain derivative method for determining the transverse shear force has been used. It is a development of the method by Cunningham [6]. Cunningham's work focused on the output from two gauges, while the method used here considers the strain from a series of gauges. The work here also builds on the previous work by the authors in this area [7,8].

A 1030 × 600 mm test specimen, with aluminium skins and an aramid honeycomb core, was manufactured for testing in a custom built Servo-hydraulic Slam Testing System for testing under water impact conditions. In addition to the panel, a beam specimen was manufactured measuring 600 mm long × 60 mm wide for experimentally obtaining the flexural stiffness and validating the strain derivative method.

The purpose of using aluminium rather than composite skins was to reduce the variability in strain measurement by using a homogeneous skin material. Previous attempts to use a strain derivative method on composite skins during slamming impacts in the SSTS were not successful due to scatter in the strain data when only considering a single pair of gauges [8]. The reason behind this was determined to be the micro-scale variations in the material properties of the composite skins leading to local spatial variations in the strain measurements. One option to improve the method would be to use strain gauges with a longer and/or wider sensor area. An increase in length however would reduce the accuracy of the method by increasing the averaging effect of each gauge. The other option, which was chosen, was to select a material without significant micro-scale variations in properties in order to develop and validate the method.

Hydroelasticity has been shown to vary the pressure distribution during slamming of flexible panels [9]. This variation will lead to a change in the transverse shear and bending moment distributions along the panel, therefore deformation should be kept to a minimum in this work to prevent significant variations with increasing impact velocity. A maximum deflection of 1.5% of span was selected for the testing. Stenius et al. [10] concluded that below 2% hydroelasticity was insignificant. Restricting deflection to below 1.5% will also ensure the deformations do not become significantly non-linear and membrane stress are negligible for a simply supported panel.

2. Test specimens

Details of test specimens are outlined in Table 1. In preparing the specimens the aluminium skins were bonded to the core using SA 70 epoxy adhesive film. The skins, adhesive film and core were stacked in order and placed under vacuum on a flat mould. The adhesive was then cured in an oven following the prescribed cycle time of a 40 min ramp to 82 °C, held at 82 °C for 3 h then cooled to 20 °C over 60 min.

The panel and beam were instrumented with strain gauges at the positions shown in Figs. 1 and 2 respectively. The specifications of the gauges are given in Table 2. All the gauges were aligned across the short span of the panel and along the length of the beam. The gauges located at location B on the beam and S5 on the panel are a single gauge with a linear array of sensors. These gauges (EA-06-031MF-120) come in a pre-fabricated array of 10. For the purposes of identifying the gauges at S5, they have been denoted C1–C10 in this work. C10 being closest to the outer edge of the panel. At location C a gauge is adhered to both the upper and lower surface of the beam in order to check the location of the neutral axis and that the strain is not affected by the boundary conditions. This also gives a measure of the symmetry of loading when compared with the strains at location B.

3. Experimental bending moment

Different load distributions will result in differing distributions of bending moment in the structure. A uniform pressure based slamming design load will give a distribution of bending moment symmetrical about the panel centre with the maximum bending moment at the centre of the panel for simply supported boundary conditions. Understanding the bending moment distribution and maximum bending moment in slamming impacts is important for optimising materials specifications and preventing structural failure.

The bending moment, M_x, can be determined from the measured strains using Eq. (4) [11]. This is only applicable for small deformations and no in-plane loads, which is the case for a simply supported plate with small deflections.

$$M_x = \frac{D}{1 - v_{xy}v_{yx}}\left[\frac{\partial^2 w_b}{\partial x^2} + v_{yx}\frac{\partial^2 w_b}{\partial y^2}\right] \tag{4}$$

Table 1
Details of panel and beam specimens.

Skin material	Al 5052 H34
Core material	HRH-10-3/8-3.0
Skin thickness	0.9 mm
Core thickness	18 mm
Flexural rigidity	11,250 Nm
Shear stiffness	1670 kN/m
Mass	8.0 kg/m^2

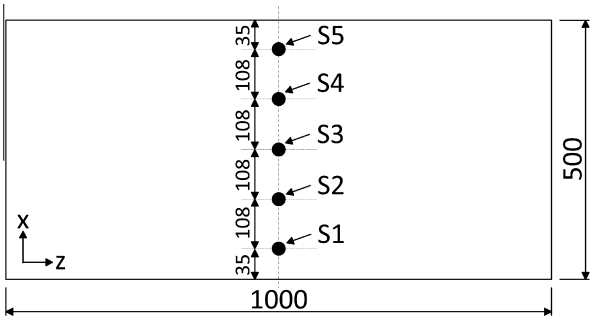

Fig. 1. Schematic of strain gauge layout on panel (dimensions in mm).

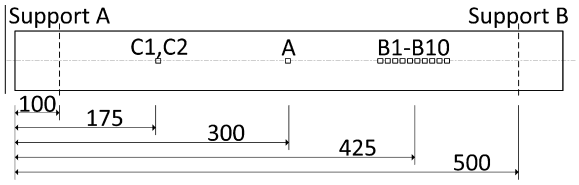

Fig. 2. Schematic of strain gauge layout on beam (dimensions in mm).

Table 2
Strain gauge specifications.

	Model	Length [mm]	Resistance [Ω]	Gauge factor
A	EA-06-060LZ-120	1.52	120 ± 0.3%	2.04 ± 0.5%
B	EA-06-031MF-120	10 × 0.79	120 ± 0.5%	2.05 ± 1.0%
C	EA-06-060LZ-120	1.52	120 ± 0.3%	2.04 ± 0.5%
S1–S4	SGD-6/120-RYB81	6.0	120 ± 0.3%	2.13 ± 0.3%
S5	EA-06-031MF-120	10 × 0.79	120 ± 0.5%	2.05 ± 1.0%

4. Strain derivative method

The transverse shear force can be estimated using the strain derivative theory developed by Cunningham [6]. Cunningham's work utilised the difference in measured bending moment, based on measurements from a pair of strain gauges, to determine the applied transverse shear force. The formula for estimation of shear force by Cunningham is given in Eq. (5). The formula is for calculation of the shear force in a beam with a width of b, at location x, half way between two strain gauges.

$$T_{xy}(x) \approx \frac{D}{bdz}\frac{\in_{x(x+\Delta x/2)} - \in_{x(x-\Delta x/2)}}{\Delta x} \tag{5}$$

The precision of the method is dependent on the measurement accuracy of the gauges, the distance between and the gauge length. The effect of an increase in either the distance between the gauges or the gauge length is an increase in the averaging of the shear force estimation. This will not substantially affect the result if the strain increases linear or is constant in the region being considered, such as a 4-point loaded beam, as used by Cunningham for validation. More significant errors will result in scenarios where there is a non-linear shear distribution, as predicted in slam loaded panels [9].

For a panel, the calculation of the transverse shear force is given by Eq. (6). By combining Eqs. (5) and (6), Eq. (7) gives an estimation of the relationship between the strain measured at two locations on the surface of a panel and the transverse shear force at a location half way between these two gauges.

$$T_{xy} = \frac{D}{1 - \nu_{xy}\nu_{yx}}\left[\frac{\partial^3 w_b}{\partial x^3} + \nu_{yx}\frac{\partial^3 w_b}{\partial x \partial y^2}\right] \tag{6}$$

$$T_{xy}(x) \approx \frac{D}{1 - \nu_{xy}\nu_{yx}}\left[\frac{(\in_{x(x+\Delta x/2)} + \nu_{yx}\in_{y(x+\Delta x/2)}) - (\in_{x(x-\Delta x/2)} + \nu_{yx}\in_{y(x-\Delta x/2)})}{x}\right] \tag{7}$$

Estimation of the shear force in this work is to be undertaken at locations B on the beam specimen and S5 on the panel specimen. At each of these locations a series of 10 gauges have been applied, with a distance between the gauges of 2 mm and a gauge length of 0.79 mm. The gauge spacing and length have been kept as low as practical to reduce the averaging effects as much as possible. As a result of such small gauges and spacing the difference in strain between the each of the gauges is expected to be less than 10% based on the estimated magnitude of the transverse shear force. The combined resistance and gauge factor error as specified by the gauges' manufacturer, Vishay Micro-measurements, is ±1.5%. Therefore if an adjacent pair of gauges were to be used for determining the shear force it is possible that an error of up to 30% could be present. This large possible error will generate significant variation in shear force estimation.

A development of this method is to use a series of gauges to determine the distribution of bending moment. This distribution can then be differentiated in order to establish the shear force distribution. This differentiation can either be done over the entire length of a panel for sparsely distributed gauges, such as S1–S5 on the panel as shown in Fig. 1, or across a cluster of gauges, such as those located at S5.

Initially the distribution of bending moment can be determined by calculation of the bending moment at each strain gauge using Eq. (5). Curve fitting is then undertaken on these values. An assumption of the order for the curve to be fitted needs to be made. For a simply-supported panel with a uniformly distributed pressure applied, the resulting bending moment fits a 2nd order polynomial. The load distribution in slamming events has been approximated by previous researchers as exponential [12]. In order to better capture the non-uniformity in the pressure distribution, a higher order polynomial should be selected for fitting of the calculated moments. For this work a 4th order polynomial has been selected. A 4th order polynomial curve fit of the bending moment results in a 3rd order trend line for the estimated transverse shear force. In this work MATLAB's *Polyfit* function has been used to undertake the curve fitting using linear regression. The equation for this curve can then be differentiated to estimate the transverse shear force.

5. Static beam testing

The beam specimen was tested in an Instron 1186 testing machine using a four point bend fixture. The beam was loaded up to 5 mm displacement of the loading points with a cross-head speed of 5 mm/min. The major span was set to 450 mm and the minor span set to 150 mm. Fig. 3 shows the beam specimen in the four point bend fixture. The wires attached to the strain gauges are visible. It can be seen that the gauges at locations A and B are located on the lower side of the beam.

The flexural rigidity, D, was determined from the measurement of the strain in gauge A and the force from the load cell. Flexural rigidity, D, is calculated using Eq. (8), where M is the bending moment, which is based on simple beam theory and symmetric four point loading, z is the distance between the neutral axis and the strain gauge and ε is the strain in the long direction of the beam as measured by the strain gauge. The flexural rigidity calculated from the test results was 11,250 Nm.

$$D = \frac{Mz}{\varepsilon} \tag{8}$$

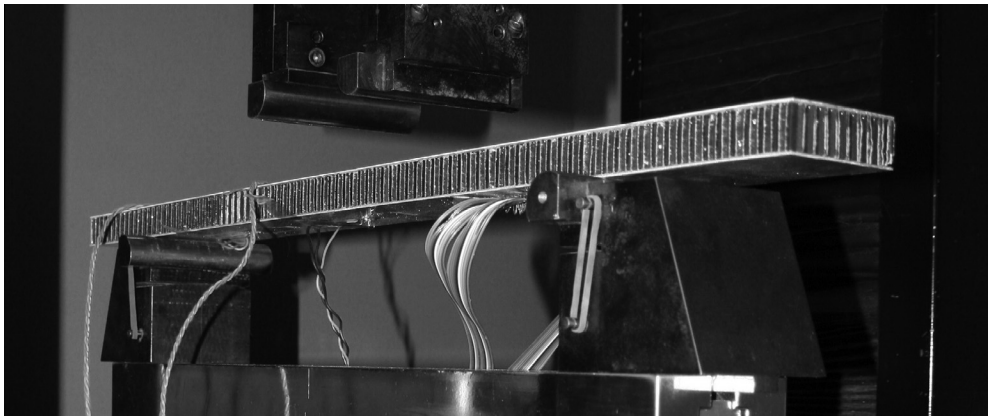

Fig. 3. Beam specimen in the four point bend fixture with strain gauges and wiring attached.

A comparison between C1 and B6 indicated loading of the beam was within 2% of being symmetrical, while the comparison between C1 and C2 indicated the absolute strains on either face of the beam are within 14%. The load on the beam is sufficiently close to being symmetrical about the load points, the difference between the top and bottom of the beam is a little higher, and therefore it must be considered as a possible source of error in the strain derivative method estimation. It is possible that either there is some membrane stress present in the beam or more likely the neutral axis is not along the centreline of the beam. Strains measured at location B were used to estimate the applied shear force during the testing.

The correlation between the shear forces obtained from the strain derivative method and the load cell is good, although reduces as the deflection increases, with a maximum variation across the range tested of 10%. It is possible that there is some effect of the asymmetry in the load distribution as well as geometric nonlinearity as the deflection increases. The maximum deflection, 4.16 mm, equates to 20.8% of the beam thickness and 1.04% of the 400 mm span. Considering the level of errors in the measurement, the simple beam theory assumptions involved, possible asymmetric loading or geometric nonlinearities involved as the deflection increases, this level of correlation is seen as sufficient.

6. Experimental slam testing

The system used in this study for testing the panel specimen is known as the Servo-hydraulic Slam Testing System (SSTS). This was custom designed and developed by Industrial Research Limited, Auckland, NZ and the University of Auckland, NZ. It utilises a sophisticated high-speed servo-hydraulic system to control the motion of a panel structure during impact with the water. It can be programmed to have a constant velocity throughout the slam event, or to follow a changing velocity profile such as may be measured on a real vessel or predicted by motion prediction software.

Tests were undertaken with a deadrise angle of 10° and nominal impact speeds ranging from 1.0 m/s to 3.5 m/s with 0.5 m/s increments. During the impacts the applied load and corresponding panel responses are measured and recorded using a variety of load cells, strain gauges and displacement transducers along with a high speed data acquisition system. Further details of the system and its performance can be found in Battley and Allen [13].

6.1. Panel deflections

In order to determine the linearity of the panel deformations and restrict any hydroelasticity that may be occurring, the deformations of the panels were measured during the testing. The deflection of the panel was measured at two locations using LVDTs mounted to the test fixture rig and in contact with the dry surface of the panel. D3 is measured at the same location as S3, close to the centre of the panel. D5 is measured at the same location as S5, close to the chine edge of the panel in the middle of the long span. The maximum deflections for each of the tests are given in Fig. 4. The largest deflection, 6.5 mm, occurs at the centre of the panel. This level of deflection is equivalent to 32.5% of the panel thickness and 1.3% of the span. At this level of deflection geometric nonlinearities are expected to be minor and are therefore assumed negligible. This relative level of deflection is similar to that seen in the static beam testing.

6.2. Maximum bending moment

For a simply supported panel with an aspect ratio of 2 with a uniformly distributed load the magnitude of the maximum bending moment in the x and z direction are given by Zenkert [11] as Eqs. (9) and (10) respectively.

$$M_x = 0.1017qb^2 \tag{9}$$

$$M_y = 0.0464qb^2 \tag{10}$$

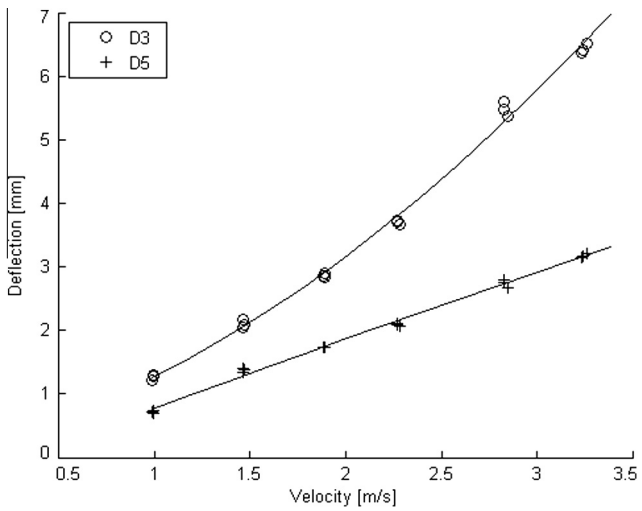

Fig. 4. Maximum measured deflections at the centre, D3 and the chine D5 (2nd order polynomial curve fits).

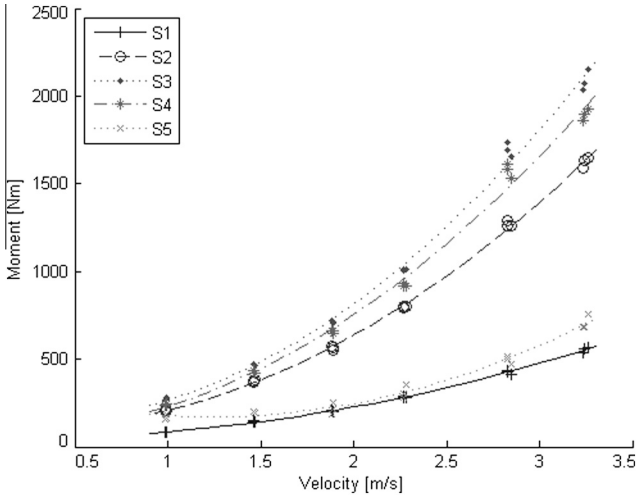

Fig. 5. Peak moments in the *x*-direction measured at the strain gauges locations on the Al-Nom panel.

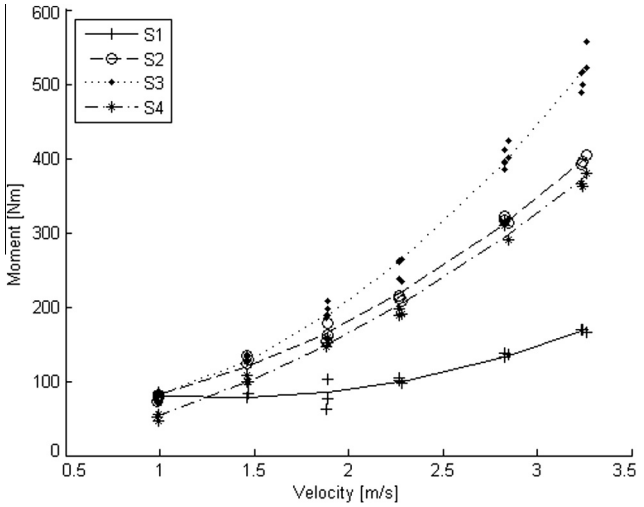

Fig. 6. Peak moments in the *z*-direction measured at the strain gauges locations on the Al-Nom panel.

Experimentally determining the maximum bending moment is difficult as measurements of strain are only taken at discrete positions that may not correspond with the actual maximum. The peak moments based on the strains measured on the panel are presented in Figs. 5 and 6 respectively. The largest measured peak moment values for both M_x and M_z occur at the centre of the panel (S3), however if the maximum moment on the panel occurred at S3 the measured values of peak moment at S2 and S4 would be expected to be the same. For M_x the moment at S4 is substantially higher than S2, indicating that the maximum M_x occurs somewhere between S3 and S4, not at S3 as predicted for a uniformly distributed load. This illustrates the effect of the non-uniform distributed load experienced during slamming. Peak measurements of M_z at S2 and S4 however are much more similar, suggesting the maximum M_z occurs close to S3.

The strain measurements indicate that for most impacts the maximum bending moment in the x direction occurs somewhere between S3 and S4. In order to obtain a value for the maximum bending moment the measured data was curve fitted with a fourth order trend line and an approximation of the maximum obtained. The order of the polynomial was selected to match the theoretical deformed shape of a panel under a distributed load. The form of the polynomial is given in Eq. (11); where p_1 to p_5 are obtain through a least-squares best fit approach.

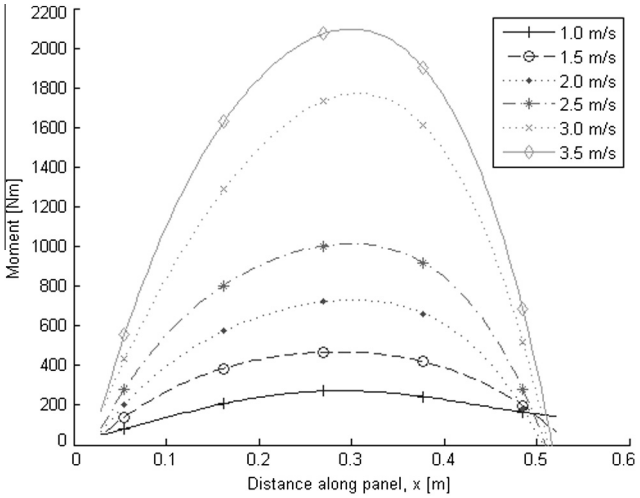

Fig. 7. Peak measured M_x moments from the panel with curve fitted lines.

$$M_x(x) = p_1x^4 + p_2x^3 + p_3x^2 + p_4x + p_5 \tag{11}$$

Fig. 7 plots the peak measured moments across the panel for impacts at six different velocities. As anticipated the maximum M_x bending moments do all occur between S3 ($x = 0.270$) and S4 ($x = 0.378$). The magnitudes of the maximum bending moments, obtained from the fitted curve, are; 208, 369, 553, 792, 1353 and 1667 Nm for 1.0–3.5 m/s respectively.

The maximum bending moments in the *x* direction, obtained from the curve fitting shown in Fig. 7, are shown in Fig. 8 along with design predictions. These predictions are based on a uniformly distributed load with the magnitude given by Wagner [2] (Eq. (2)) and von Karman [3] (Eq. (3)) with the moment calculated from Eq. (9). The experimentally obtained values are significantly below the predictions based on Wagner, however are very similar to the predictions based on von Karman.

An alternative approach to determining the maximum bending moment is to curve fit the bending moments for each time step. Fig. 9 presents bending moments at five time steps for a 2.0 m/s impact. It is clear that as the time progresses and the panel becomes further submerged the maximum bending moment

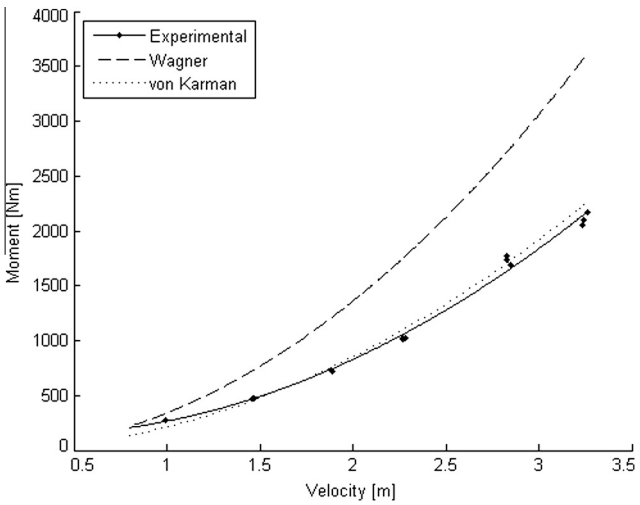

Fig. 8. Experimental maximum moments in the *x* direction compared with analytical predictions.

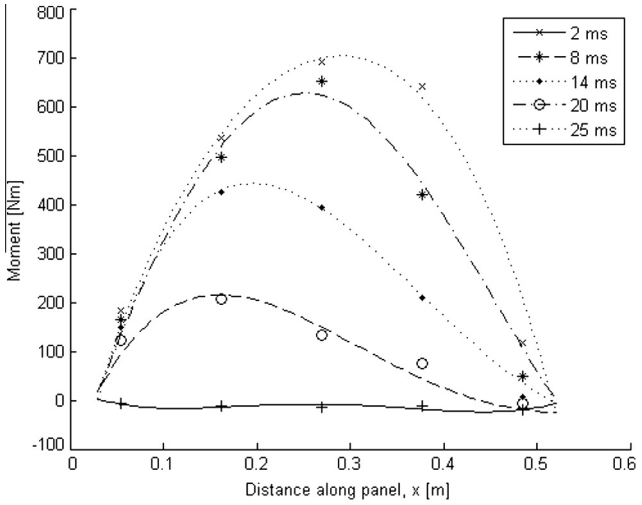

Fig. 9. Experimental bending moments in the x direction at various times for 2.0 m/s impact.

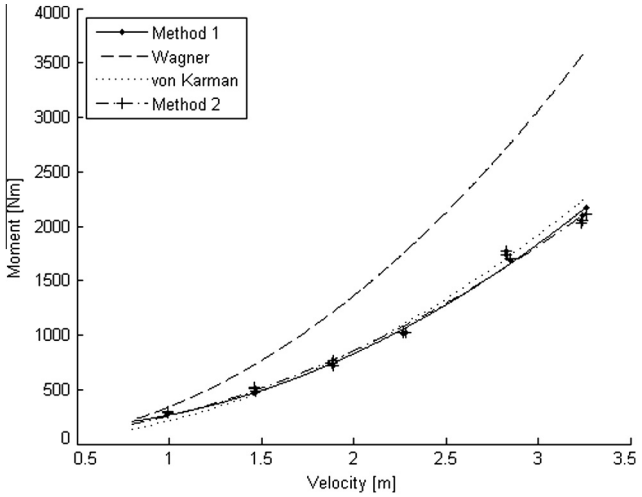

Fig. 11. Maximum experiment bending moments for both experimental estimation methods as well as analytical predictions.

increases and shifts towards the chine edge of the panel (x = 0.520 m).

If the maximum bending moment is taken from each of the time steps for each impact the maximum bending moment during the impact can be estimated. Fig. 10 presents the time histories of maximum bending moments calculated from each time step, as shown in Fig. 9. From these time histories it is then also possible to determine an estimation of the maximum bending moment during each impact.

Fig. 11 compares the maximum bending moment for each of the impacts calculated using both of the above methods as well as the analytical predictions based on both Wagner and von Karman. It is clear that there is little variation between the two methods for estimation of the maximum bending during the experimental impacts; the two trends lines are almost identical. The first method, basing it off the maximum bending moment at each strain gauge location, is significantly less computationally intensive as it only requires one curve fitting per impact.

6.3. Maximum shear force

As discussed earlier the strain derivative method can be implemented using either a pair or series of strain gauges. Fig. 12 plots the strain measured at S5 for all 10 gauges for an impact at 3.5 m/s with a deadrise angle of 10°. C1 is the gauge closest to the centre and C10 is the gauge closest to the chine edge of the panel. C1 and C10 are 44 and 26 mm respectively from the boundary, with the 2 mm spacing between each of the 10 sensors. At all velocities there is a general trend of decreasing strain from C1 to C10. Impacts where C2 is higher than C1 or C9 is lower than C10 highlight the difficulties of simply selecting a pair of gauges to use for transverse shear force estimation. Utilising a series of gauges will result in a more accurate estimation of shear force as local variation and strain gauge measurement errors will be less influential.

S5 is located near the centre of the long edge such that it should be close to the maximum transverse shear force, which is predicted to be close to the chine edge of the panel. In order to obtain the transverse shear force, the moment in the x direction is differentiated with respect to x, as shown in Eq. (12), where M_x has been obtained from Eq. (11). This differentiation results in Eq. (13), where constants p_1–p_4 have been obtained from the previously undertaken least squares best fit. The transverse shear force at S5 (x = 0.485 m) can then be obtained from Eq. (13). As was done for the bending moment, this is calculated for each time step to produce a time history of the transverse strain at S5.

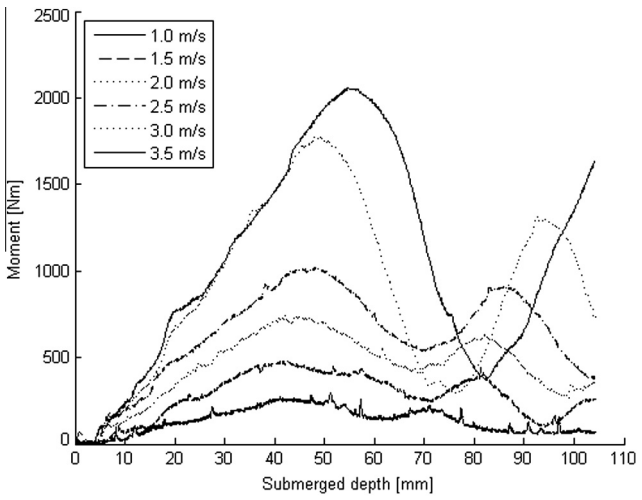

Fig. 10. Maximum experiment bending moments in the x direction versus submerged depth of the panel.

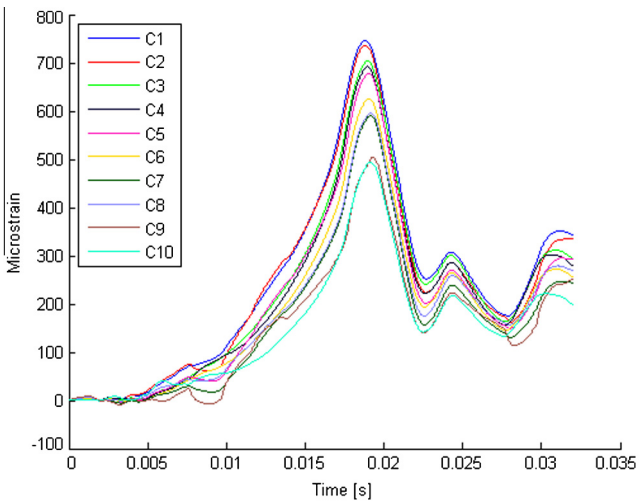

Fig. 12. Chine strains (S5) measured on the panel for 3.5 m/s, 10° impact.

$$T_x(x) = \frac{\partial M_x}{\partial x} \tag{12}$$

$$T_x(x) = 4p_1x^3 + 3p_2x^2 + 2p_3x^1 + p_4 \tag{13}$$

Fig. 13 presents the calculated transverse shear force at S5, based on the strain derivative method, for a range of impacts. As expected there is an increase in the magnitude of the transverse shear force with increasing impact velocity. Interestingly the peak transverse shear force occurs progressively later in the impact as the impact velocity increases.

The maximum from each of these time histories can be used to establish a relationship between impact velocity and maximum transverse shear force at S5 for 10° impacts. The time histories presented in Fig. 13 are based on all of the gauges, S1–S5 as well as C1–C10. It is possible to undertake the same calculations based on any set of gauges, for instance only S1–S5 or C1–C10. Fig. 14 presents the maximum transverse shear forces calculated from all the strain gauges, gauges S1–S5 and gauges C1–C10.

The predictions based on Wagner and von Karman are also presented, similarly to Fig. 11. The analytical solutions for the maximum shear force are calculated from Eq. (14), where q is the equivalent uniform load obtained from Wagner and von Karman.

$$T_x = 0.465qb \tag{14}$$

Shear forces based on S1–S5 are the lowest of the experimental values, also lower than both of the analytical predictions. The more significant the influence of the gauges at located at S5 the higher the shear force estimation. When only the gauges at S5 are considered (C1–C10) the shear force estimation is the highest.

6.4. Maximum shear to bending ratio

The maximum bending moments and shear forces have been compared with predictions based on uniformly distributed loads with magnitudes given by Wagner and von Karman. The experimental bending moments were very similar to those based on von Karman's pressure formulation. The maximum shear force depended on which set of gauges were considered. The more influence the gauges located at S5 had, the greater the shear force estimation was, to the point that the estimated shear force was approximately the same as that based on Wagner's pressure calculation which is 1.57 times greater than that based on von Karman's pressure.

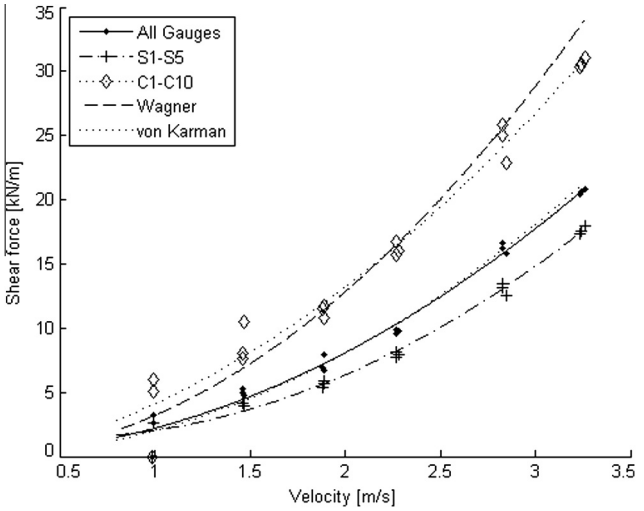

Fig. 14. Maximum experimental transverse shear force at (S5) compared with analytical predictions.

While it would be possible to simply increase the magnitude of the von Karman pressure applied in order to sufficiently predict the shear force magnitude, doing so would significantly over predict the bending moment, resulting in a sub-optimal structure. There the ratio between the maximum shear force and bending moment, as defined in Eq. (15), should be considered.

$$R_{T:M} = \frac{T_{x,max}}{M_{x,max}} \tag{15}$$

For a simply supported panel with a uniformly distributed load, an aspect ratio of 2 and an unsupported width of 485 mm, the analytical solution for the ratio between the maximum shear force and maximum bending moment ratio is 9.43 [11]. This ratio is compared with the values for $R_{T:M}$ obtained from the panel slamming experiments in Fig. 15.

Experimentally the ratio varies depending on which set of gauges has been used. For 'all gauges' the average ratio is 9.72, only 3.11% higher than the analytical ratio for a simply supported panel. The average ratio based on S1–S5 (with the less influence of the gauges at S5) is 8.02, 15.0% lower than the analytical ratio. Finally the average ratio based on C1–C10 is 15.90, 68.7% higher than the

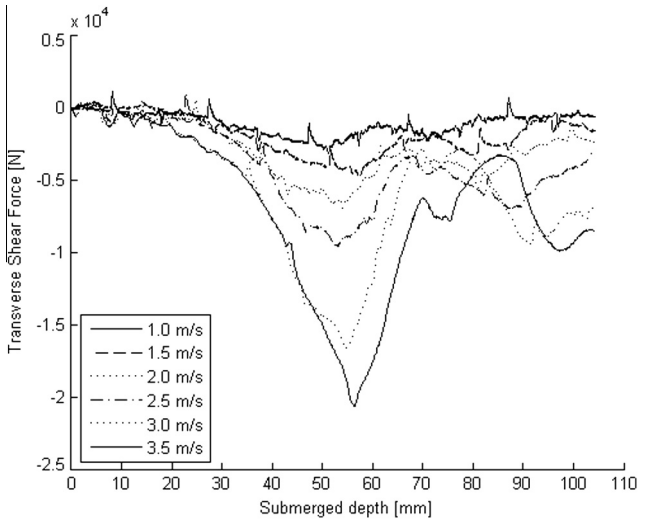

Fig. 13. Time history of transverse shear force at (S5) obtained using strain derivative method.

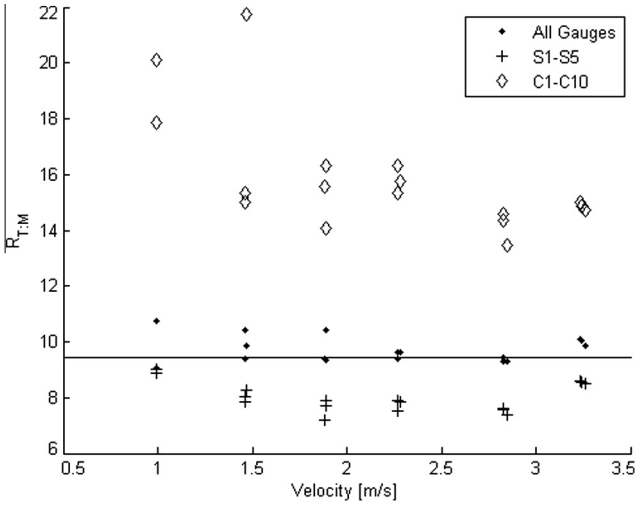

Fig. 15. Experimental $R_{T:M}$ values compared with analytical prediction of 9.43 (solid line).

analytical ratio. There are some variations in the ratios with increasing impact velocity, however it appears mostly that at low velocities the ratio is higher, which may be simply increased errors in the estimation method when the absolute strain values are smaller.

7. Conclusions

A strain derivative for determining transverse shear force has been successfully validated using a beam subjected to 4-point loading. In order to improve reliability and accuracy the method has been extended to use a linear trend line across a series of gauges. This method has again been further extended to higher order polynomial trend line fits and applied to a 1000 × 500 mm panel tested under controlled velocity water impacts.

Estimated maximum experimental bending moments and the transverse shear force at the chine edge (S5) for the panel impacts have been compared with predictions based on analytical solutions for equivalent uniformly distributed loads. The analytical solutions were based on pressures based on von Karman and Wagner's works.

Two different approaches were identified and used for estimation the maximum bending moment. Both methods corresponded well with each other and have been shown to be approximately equivalent to the predictions based on the equivalent uniform pressure solution of and von Karman.

Estimation of the transverse shear force has been undertaken using differing sets of strain gauges. The greater the proportion of gauges in the set located at S5, the higher the estimated transverse shear force was shown to be. If only those gauges located at S5 were considered for estimation of the transverse shear force, the resultant magnitude was approximately 65% higher than the prediction based on von Karman, making it a similar magnitude to the prediction based on Wagner.

The ratio between the maximum bending moment and the transverse shear force at S5 has also been considered. As while it would be possible to scale up pressure predictions in order to accurately capture the maximum transverse shear force, this would result in an over predicted bending moment and likely a sub optimal design. When all of the gauges were considered, 5 across the panel and 10 clustered at S5, the bending to shear ratio closely matched the analytical ratio of 9.43. Just considering the 5 gauges across the width of the panel resulted in a reduction of shear to moment ratio of 15.0%. If only the gauges located at S5 where considered, the ratio increase to 68.7% higher than predicted. Increasing the influence of the gauges located at S5 would likely result in the most accurate prediction of transverse shear at that location. It is therefore considered that the real transverse shear force is likely to be most similar to the estimation based on C1–C10, giving a shear to bending ratio 68.7% higher than the prediction.

Using a uniformly distributed load to represent the actual non-uniform slamming load will potentially lead to a non-optimised structure if the magnitude is sufficient to accurately predict the maximum shear force (based on the C1–C10 estimation) or alternatively lead to under prediction of the transverse shear force if the correct bending moment is predicted. For traditional monolithic shell structures this may not present a substantial issue as transverse shear failure is not a common failure mode, however for sandwich structures, unexpected shear failure in the core may occur. An approach may be to utilise this experimental data and add a correction factor to better represent the $R_{T:M}$ values obtained.

Acknowledgements

This research has been financially supported by the USA Office of Naval Research (Grant N00014-08-1-0136, Programme Manager Dr Yapa Rajapakse) and the NZ Ministry for Business, Innovation and Employment through contract UOAX0710. The assistance of Industrial Research Limited and Gurit is also gratefully acknowledged.

References

[1] Rules for classification of high speed, light craft and naval surface craft. In: Veritas DN, editor. 2005.
[2] Wagner H. Über Stoß- und Gleitvorgänge an der Oberfläche von Flüssigkeiten. ZAMM – Zeitschrift für Angewandte Mathematik und Mechanik. 1932;12:193–215.
[3] Von Karman T. The impact on seaplane floats during landing. National Advisory Committee for Aeronautics; 1929.
[4] Lolive E, Casari P, Davies P. Loading rate effects on foam cores for marine sandwich structures. Sandwich Struct 7: Adv Sandwich Struct Mater 2005:895–903.
[5] Burman M, Rosen A, Zenkert D. Spectrum slam fatigue loading of sandwich materials for marine structures. In: 9th International Conference on Sandwich Structures (ICSS 9)California.
[6] Cunningham PR, White RG. A new measurement technique for the estimation of core shear strain in closed sandwich structures. Compos Struct 2001;51:319–34.
[7] Allen T, Battley M. Transverse shear force during slamming impacts using a strain derivative method. 12th International Conference on Fast Sea Transportation. Amsterdam, The Netherlands.
[8] Allen T, Battley M. Experimental methods for determining shear loads in sandwich structures subjected to slam loading. In: 9th International Conference on Sandwich Structures (ICSS 9). California; 2009.
[9] Allen T, Battley M. Quantification of hydroelasticity in water impacts of flexible composite hull panels. Ocean Eng 2015;100:117–25.
[10] Stenius I, Rosén A, Battley M, Allen T. Experimental hydroelastic characterization of slamming loaded marine panels. Ocean Eng 2013;74:1–15.
[11] Zenkert D. The handbook of sandwich construction. EMAS; 1997.
[12] Zhao R, Faltinsen O. Water entry of two-dimensional bodies. J Fluid Mech 1993;246:593–612.
[13] Battley M, Allen T. Servo-hydraulic system for controlled velocity water impact of marine sandwich panels. Exp Mech 2011;1–12.